Available online at www.sciencedirect.com

ScienceDirect

journal homepage: www.elsevier.com/locate/he

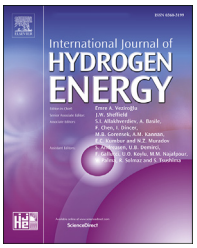

Electrochemical low-frequency impedance spectroscopy algorithm for diagnostics of PEM fuel cell degradation

Ivar J. Halvorsen [a,*], *Ivan Pivac* [b], *Dario Bezmalinović* [b], *Frano Barbir* [b], *Federico Zenith* [a]

[a] *SINTEF Mathematics and Cybernetics, Klæbuveien 153, Trondheim, Norway*

[b] *Faculty of Electrical Engineering, Mechanical Engineering and Naval Architecture, University of Split, Ruđera Boškovića 32, Split, Croatia*

ARTICLE INFO

Article history:
Received 7 September 2018
Received in revised form
28 March 2019
Accepted 1 April 2019
Available online xxx

Keywords:
Fuel cell
Diagnostics
Prognostics
Relay feedback
Impedance

ABSTRACT

Prognostics and health management for fuel cells in real-world applications are important for optimization of lifetime and operation. A parameter that has been shown to indicate the state of ageing is the low-frequency intercept with the real axis of the Nyquist diagram in a fuel cell's impedance spectrum. This article presents a method for direct identification of this parameter, without the need to carry out a full electrochemical impedance spectroscopy, and with an algorithm that can be realized within a typical fuel-cell control system. The proposed method is based on relay excitation feedback, a proven solution from controller tuning.

Introduction

Proton-exchange membrane (PEM) fuel cells are today the most popular type of fuel cells, and are employed in automotive, stationary and portable applications. The focus of much research in fuel cells in later years has been on reducing production costs and increasing lifetime, to reduce the total cost of ownership of fuel cells [1]. Durability, as the one of the main shortcomings of this state-of-the-art, zero-emission power technology, limits a faster commercialisation, and many studies are devoted to early detection of the degradation symptoms and identification of the causes and degradation mechanisms [2–5].

Nowadays, a popular laboratory technique for investigation of the degradation state of fuel cells is electrochemical impedance spectroscopy (EIS) [6–11]. It is a well-established diagnostic method in form of transfer function analysis, which allows processes occurring with different time constants to be identified and distinguished due to different loss mechanisms by analysing the cause/effect relationship between a small sinusoidal perturbation of current or voltage

* *Corresponding author.*
E-mail addresses: Ivar.J.Halvorsen@sintef.no (I.J. Halvorsen), ipivac@fesb.hr (I. Pivac), dbezma@fesb.hr (D. Bezmalinović), fbarbir@fesb.hr (F. Barbir), Federico.Zenith@sintef.no (F. Zenith).

https://doi.org/10.1016/j.ijhydene.2019.04.004

applied to a system and its consequences. Furthermore, impedance is monitored even in the control system of the fuel-cell car Toyota Mirai [12]. There are also a few novel transfer-function diagnostic techniques as EIS variations, such as electro-thermal impedance spectroscopy (ETIS), which uses the relationship between current perturbation (load on the fuel cell) and the consequent temperature change/heat generation, to map fuel cell operation [13], and electrochemical pressure impedance spectroscopy (EPIS), which uses the relationship between the sinusoidal perturbation of reactant cathode pressure and cell voltage response to determine low-frequency processes at lower capital cost and gain deeper insight into the mass transfer effects associated with a hydration imbalance as complementary information to EIS [14]. However, EIS in general cannot be deployed in commercial applications because of the size and cost of the required equipment, the duration of the tests, and not least the complexity of the results, which require highly trained personnel to interpret and act upon.

Rezaei Niya et al. [15] performed a study connecting first-principle models and EIS equivalent circuits, and for the "low-frequency arc" they found that data published in literature was consistent with dependence on phenomena related to humidification: in particular, the low-frequency arc first shrinks with increasing current, but inflates again close to the mass-transport barrier; it inflates in dry-out conditions, and it "retracts" when the cathodic gas-diffusion layer (GDL) is flooded (i.e. the intercept with the real axis in the EIS plot has a significantly lower frequency).

Pivac et al. [16] presented an extended interpretation of PEM fuel cell impedance spectra by introducing a resonant circuit in the equivalent-circuit model associated with the mass transport process (i.e. reactant gas diffusion in water/ionomer in catalyst layer), as shown in Fig. 1, to calculate its parameters under a variety of operating condition. As each impedance spectrum consists mainly of a small high-frequency (4 kHz–0.6 kHz) capacitive loop, a medium-frequency (600 Hz–8 Hz) capacitive loop and a low-frequency (8 Hz–0.2 Hz) capacitive loop followed by an inductive loop at the lowest frequencies (0.2 Hz–0.01 Hz) [16], their equivalent-circuit model was based on their previous review of inductive phenomena in fuel cell impedance spectra at low frequencies [17] to capture these inductive loops as well. The low-frequency capacitive loop moves toward the real axis indicating a finite length of charge diffusion in the fuel cell and it is related to mass transport/diffusion processes [18], i.e. contribution of oxygen concentration gradient in the cathode. Therefore, the mass transport impedance is observed at lower frequencies because it takes time for the reactants to move and penetrate farther into the catalyst layers and gas diffusion layers at both electrodes, resulting in a higher diffusion resistance value [18,19]. In their follow-up paper [11], they performed repeated studies on how parameters of this 11-element model changed during accelerated stress tests.

They found that one of the parameters, the resistance in the cathode resonant circuit (R_4 in Fig. 1), was linearly changing with degradation (i.e. voltage cycles of the accelerated electrocatalyst degradation test), and was therefore a good candidate *prognostic variable*, i.e. a variable from which the degradation state of the cell can be easily assessed. The cathode catalyst layer resistance (R_4), representing resistance to oxygen supply (i.e. diffusion of oxygen inside polymer in the cathode catalyst layer) [16], increased with degradation caused by Pt dissolution, which is associated with the diffusion (i.e. permeation rate) decrease with degradation [11]. The resistance in the resonant circuit, however, is in parallel with an inductance, meaning that at steady state it is "shorted out" and not measurable: any measure of this variable will require some sort of dynamic operation. Recently, Ren et al. [20] have applied the same equivalent circuit model (with the constant phase element instead of the cathode double layer capacitance to improve the fitting quality) as indicator of water flooding at low frequencies.

While EIS would be the obvious candidate method in a laboratory, it is not deployable in commercial applications. Therefore, faster methods based on EIS approach [21–25], coupled with algorithms that estimate/measure impedance response at certain frequencies [26], are required for low-cost on-line implementation of an efficient degradation diagnostic tool within an embedded fuel cell control system. To ameliorate the shortcomings of EIS in commercial applications, Jeppesen et al. [21] proposed a method based on *current pulse injection* to estimate fundamental EIS parameters, but the method admittedly neglected the lower-frequency arcs of the spectrum and focused on the high and intermediate frequencies. Furthermore, Brunetto et al. [22] proposed a multi-sine approach, where the fuel cell under test is perturbed

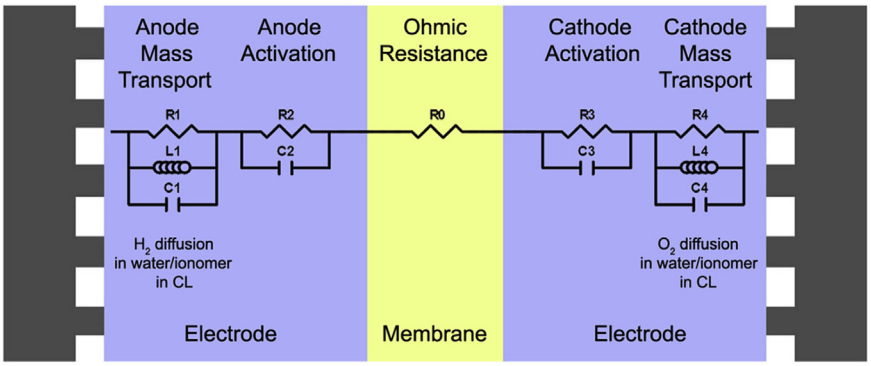

Fig. 1 – The extended equivalent circuit proposed by Pivac et al. [16], featuring two additional resonant circuits on the sides.

Please cite this article as: Halvorsen IJ et al., Electrochemical low-frequency impedance spectroscopy algorithm for diagnostics of PEM fuel cell degradation, International Journal of Hydrogen Energy, https://doi.org/10.1016/j.ijhydene.2019.04.004

with a signal composed of multiple sinusoids, hence economising the required measurement time, but this requires additional measurement equipment and it is also limited in the low frequency region, where fuel cell degradation is most visible [11]. Debenjak et al. [26] developed a low-cost impedance measurement system for measuring impedance only at certain frequencies to separate the normal, flooded and dried state of the fuel cell system, which is feasible for direct installation in commercial systems. Debenjak et al. [24] presented also a novel EIS approach for fast measurement of the PEM fuel cell impedance, which utilizes a Pseudo-Random Binary Sequence (PRBS) as a perturbation signal for further fuel cell diagnostic purposes, where the impedance is estimated by using Continuous Wavelet Transform (CWT) with Morlet mother wavelet at any frequency band of interest with properly tuned CWT parameters. However, it has higher uncertainty at low frequency region and requires a high computational burden, thus reducing its applicability on low-cost digital embedded devices. Manganiello et al. [23] overcome this issue with the approach based again on the PRBS, but with a simpler elaboration algorithm based on suitable data filtering, Fast Fourier Transform (FFT) and smoothing techniques. However, their validation and applicability did not include degradation issues. Recently, Aroge and Barendse [27] developed the idea of a low-cost active load which may be controlled by input voltage signals, helping to implement a load modulation technique to replace expensive frequency response analyser (FRA) for galvanostatic impedance measurements as a portable alternative for online diagnostics. Furthermore, they also proposed a novel technique for rapid online impedance estimation with the time-frequency analysis of the frequency-rich logarithmic chirp signal using the CWT as an analysis tool of choice implemented with an active load [25].

Two consecutive EU projects, D-CODE and HEALTH-CODE (respective IDs 256673 and 671486), focused on the possibility of integrating EIS sampling into the DC/DC converter connected to the fuel cells, along with other online diagnostics; see for example the work of Petrone [28] (D-CODE) and Russo et al. [29] (HEALTH-CODE) for an overview of their results.[1]

This article will present a simple, cheap, fast, self-correcting algorithm, so-called electrochemical low-frequency impedance spectroscopy (ELFIS), to estimate this prognostic variable with minimum disruption to the underlying process. The key idea is to establish a small current perturbation at a specific frequency, at which the resistance in the resonant circuit (R_4 in Fig. 1) can be measured by the ratio of the perturbed voltage and current measurements; a challenge is that this frequency is initially unknown and must be identified. This problem is analogous to finding the ultimate (or critical) frequency in a control loop for the purpose of controller tuning; a classical method for this related problem is the so-called *relay excitation feedback* [30].

[1] Note that HEALTH-CODE has not yet concluded at the time of writing, and some of their results may not yet be published pending IP protection measures.

Methods

Fuel-cell model

The fuel cell will be modelled as an impedance composed of the items laid out in Fig. 1, with the values of resistances, inductances and capacitances given in Table 1; these values are the ones given in Pivac et al. [16] at nominal conditions: 0.3 A/cm^2, 65 °C, cathodic inlet humidity 100%, cathodic stoichiometric ratio 4, operating backpressure 0.5 bar_g.

When EIS-sampling a fuel cell, current is perturbed by adding a sinusoidal signal of given amplitude and frequency, and the corresponding voltage amplitude and phase shift are recorded; the absolute value of current and voltage is not important here, but rather the deviation from the steady state. That is why the model in Fig. 1 does not need to include a voltage generator, whose effect would have been removed in this analysis.

The amplitude ratio between voltage output and current input, together with their phase difference at each sampled frequency, is expressed by an impedance that varies with frequency; this can also be interpreted as a *transfer function* between current and voltage in the context of control theory. Some such measured spectra are presented in Fig. 2. The electrical equivalent model in Fig. 1 is fitted to EIS data: some obvious points are easily identified, such as the resistance at high frequency (R_0) and at steady state ($R_2 + R_0 + R_3$).

Pivac et al. [11] noted that the value of resistance at the rightmost intersection with the real axis in Fig. 2 is the best candidate as an indicator of performance degradation in fuel cells, and termed it *low-frequency resistance* or LFR. The LFR is characterised in the EIS spectrum by having zero phase, i.e. $\angle Z(f_{LFR}) = 0$. The LFR is then found as the impedance magnitude at that frequency, i.e. $R_{LFR} = |Z(f_{LFR})|$.

Classical relay feedback

In process control, a relay is a simple element that essentially implements the signum function:

$$u = R(e) = \mathrm{sgn}(e) = \begin{cases} +1 & \text{if } e > 0 \\ -1 & \text{otherwise} \end{cases} \quad (1)$$

The relay function $R(e)$ is thereby a single-input, single-output, stateless function that is trivial to implement in software. Different amplitudes of the relay are easily implemented by multiplying $R(e)$ by the desired relay output amplitude d.

Relays have long been applied extensively in control practice, as they can be used to safely and automatically

Table 1 – Parameters of the fuel cell equivalent model in Fig. 1.

Element	Unit	0	1	2	3	4
R	mΩ.cm^2	96.4	24.4	82.7	158.8	56.2
C	mF/cm^2	0	9.0	17.2	35.1	1062.8
L	mH.cm^2	∞	34.8	∞	∞	573.2

Please cite this article as: Halvorsen IJ et al., Electrochemical low-frequency impedance spectroscopy algorithm for diagnostics of PEM fuel cell degradation, International Journal of Hydrogen Energy, https://doi.org/10.1016/j.ijhydene.2019.04.004

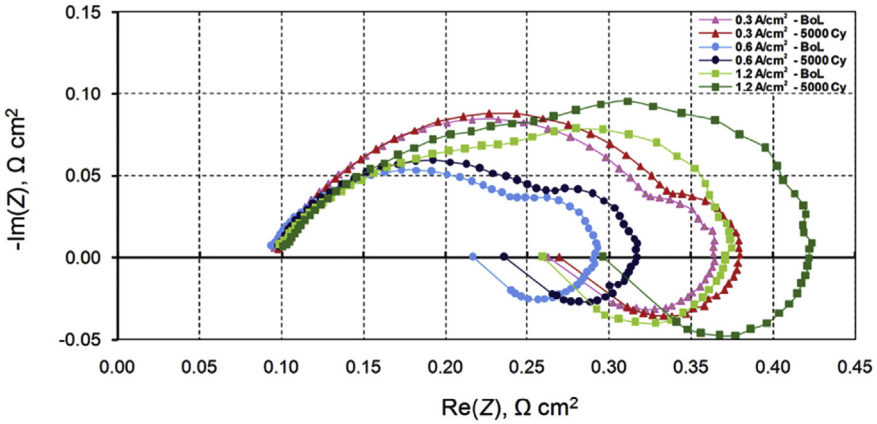

Fig. 2 – Impedance spectra for a fuel cell at 0.3, 0.6 and 1.2 A/cm², taken at Beginning of Life (BoL) and after 5000 cycles of accelerated stress testing (reprinted from Pivac et al. [11]).

measure important process parameters for controller design, i.e. the *ultimate gain* μ_u and the *ultimate frequency* f_u [§2.6 [30]].

Consider the diagram in Fig. 3, where $G(s)$ is a stable, positive-gain transfer function (s is the Laplace variable), and a relay has been placed immediately upstream the system represented by $G(s)$. As customary in process-control diagrams, all variables are assumed to be normalised so that at steady state their value is zero; reference r is assumed to remain identically zero during a relay feedback. A feedback loop is established, so that the relay input is $e = -y$.

Any small disturbance or measurement noise in y will then start an oscillation cycle, as a positive y will immediately produce a negative u, which will eventually result in a negative y, depending on the internal dynamics of system $G(s)$; the cycle will then be repeated indefinitely with a continual inversion of the relay sign.

As explained by Åström and Hägglund [30], these oscillations will eventually converge to a relay switching frequency equal to the system's *ultimate frequency* f_u, which is the frequency at which the system's input and output are in opposite phase, i.e. $\angle G(j\,2\,\pi f_u) = -180^\circ$ (where we replaced the Laplace variable s with $j\,2\,\pi f$ to obtain the frequency response).

The *ultimate gain* μ_u of $G(s)$ is defined as the gain in a P controller when the feedback system is brought to the its stability limit, that is when $\mu_u\, G(s) = -1$ (or $\mu_u\, |G(s)| = 1$). Here, the relay replaces the P controller. The effective gain of the relay is found as the ratio of the system's output and input signals at the ultimate frequency. However, since the system's input is a square wave produced by the relay, it can be decomposed into a sum of sinusoids with different frequencies (according to Fourier series analysis), and the component corresponding to f_u does not have the same amplitude d of the square wave. The gain of $G(s)$ at the ultimate frequency can then be shown to be [30]:

$$|G(j\,2\,\pi f_u)| = \frac{1}{\mu_u} = \frac{\pi\, a}{4\, d} \tag{2}$$

Where a is the amplitude of the input signal to the relay, which is fed back from the output of $G(s)$. Due to the low-pass characteristics of most processes $G(s)$, the higher-order Fourier terms produced by the relay will be dampened in the system's output, and can usually be neglected when measuring a; if it were not the case, a Fourier decomposition can be run on the output of $G(s)$ to find the amplitude a of the first harmonic sinusoidal.

Adaption of relay feedback to fuel cells

A naïve adaptation of the relay feedback on a fuel cell described by an equivalent circuit such as that pictured in Fig. 1 is shown in Fig. 4, where the fuel cell is represented by transfer function $Z(s)$, which is the composition of resistances, capacitances and inductances of Fig. 1. The input and output variables are δI and δV, which are the deviations of cell current I and voltage V from the steady-state value where the cell is assumed to be at the beginning of the test. Note that the output of $Z(s)$ is actually $-\delta V$, since an increase in current yields a *reduction* in voltage; this makes the input to the relay equal to δV after passing through the negative feedback.

The relay feedback in Fig. 4, however, does not converge to a specific frequency: it will instead switch back and forth continuously at every evaluation of the relay input, since any positive δI will immediately yield a negative δV, in turn setting a negative δI and so forth. This rapid switching is ultimately due to the fact that $Z(s)$ does *not* have a low-pass characteristic (as it was assumed in the previous section), indeed $\lim_{f\to\infty} Z(j\,2\,\pi f) = R_0$.

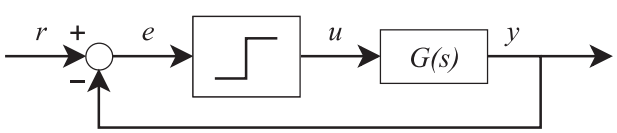

Fig. 3 – Flow diagram of a classical relay feedback loop.

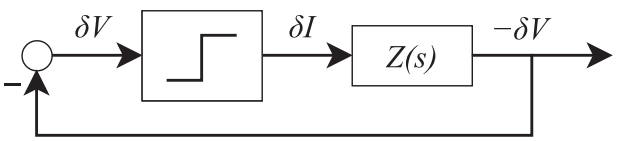

Fig. 4 – The relay feedback applied on a fuel cell.

Please cite this article as: Halvorsen IJ et al., Electrochemical low-frequency impedance spectroscopy algorithm for diagnostics of PEM fuel cell degradation, International Journal of Hydrogen Energy, https://doi.org/10.1016/j.ijhydene.2019.04.004

Furthermore, there is no ultimate frequency such that $\angle Z(j\,2\,\pi\,f_u) = -180^\circ$: as shown in Fig. 2, the impedance spectrum is wholly in the right-hand side of the complex plane, and never intersects the negative real axis. Indeed, our objective is make the relay converge to the LFR's characteristic frequency, for which we have $\angle Z(j\,2\,\pi\,f_{\mathrm{LFR}}) = 0^\circ$.

In order to filter high-frequency components and make the relay converge to f_{LFR}, we insert *two integrators* in the relay feedback loop, as shown in Fig. 5, such that $G(s)$ is replaced by $Z(s)/s^2$ when comparing to Fig. 3.

The Laplace transform of an integrator is $1/s$, meaning that integrators:

- dampen signals proportionally to their frequency;
- add to the signal a phase lag of 90° at all frequencies.

Thereby, two integrators in series strongly dampen high-frequency components, and invert the phase −180° of the input signal at all frequencies, including that of LFR:

$$\angle Z(j\,2\,\pi\,f) = 0^\circ \Rightarrow \angle\frac{Z(j\,2\,\pi\,f)}{(j\,2\,\pi\,f)^2} = -180^\circ \tag{3}$$

With such a modification, the relay feedback in Fig. 5 will then converge to a limit cycle at f_{LFR}, since by definition of LFR $\angle Z(j\,2\,\pi\,f_{\mathrm{LFR}}) = 0^\circ$. The low-frequency resistance can be found based on equation (2) when $f = f_{\mathrm{LFR}}$:

$$\mathrm{R_{LF}} = \left|Z(j2\pi f)\right| = \frac{4\,d}{\pi\,a}(2\pi f)^2 \tag{4}$$

A more direct method is to measure the deviations in the current and voltage signals, but when the signals are clearly non-linear, the first harmonics give a more correct answer.

Furthermore, integrators have minimal computational and memory requirements when implemented in software, as they need to store one single value and perform one sum per evaluation cycle.

The amplitude of the relay output is a design parameter: it should be reasonably small to minimize disruption to operation and nonlinear effects, but large enough to discriminate changes in voltage from measurement noise.

Actuator dynamics

In a real system, the dynamics of the DC/DC converter setting the cell current may be limited, or there may be specific limitations on the rate of change of current to protect the fuel cell. Such a rate limitation may be approximated with a lag with time constant τ, whose Laplace transform is $1/(\tau\,s+1)$. If τ is known, it is possible to compensate for its effect by inverting it and combining it with the integrators: the corrective term on the feedback loop then becomes:

$$\frac{\tau\,s+1}{s^2} \tag{5}$$

Which is realisable, since the denominator has higher polynomial order than the numerator. Note that this inversion requires that the actuator dynamics is a *minimum-phase transfer function*, i.e. without inverse response nor time delays, and at most a second-order lag.

In particular, time delays in the actuator may be a concern, and may induce a certain deviation in the limit-cycle frequency and in the estimation of the LFR. The phase contribution of a time delay τ_d is simply $-\tau_d\,2\,\pi\,f$, but the frequency is generally unknown at the start of the experiment. A simple solution is to use the best estimate for the design of a lead filter that can compensate with a corresponding positive phase at that frequency.

Compensation of voltage bias

When implementing relay feedback on a fuel cell, a source of uncertainty is the possibility of voltage drift: the steady-state value of voltage measured at the start of the test, which is necessary to define δV, may change gradually over time due to changes in humidity, temperature, catalyst poisoning etc. Since a criterion for low operational disruption is that oscillations should be small, even a small voltage drift may lead to asymmetric oscillation and reduce the accuracy of the estimation results: it is therefore necessary to estimate and monitor this voltage bias. In addition to this, random voltage measurement noise will also be present, so the estimation algorithm will need to be robust. We present in this section a gradient method as described by Ioannou and Sun [31], §4.3.5.

Assuming we are not too far from the LFR frequency, we have $Z \approx \mathrm{R_{LF}}$ and the following model is then valid:

$$-\delta V_m = \mathrm{R_{LF}}\,\delta I + \mathrm{V_{bias}} \tag{6}$$

Where δV_m is the modelled voltage deviation, $\mathrm{R_{LF}}$ is the estimated low-frequency resistance and $\mathrm{V_{bias}}$ is the estimated voltage bias.

The model error ε is the deviation between measured and modelled voltage:

$$\varepsilon = \delta V - \delta V_m = \delta V + \begin{bmatrix}\mathrm{R_{LF}} & \mathrm{V_{bias}}\end{bmatrix}\begin{bmatrix}\delta I \\ 1\end{bmatrix} = \delta V + \boldsymbol{\theta}^{\mathrm{T}}\,\phi \tag{7}$$

where $\boldsymbol{\theta}$ is the parameter vector and the equation has been converted to matrix form. An appropriate cost function to minimise and find the best parameter estimate is:

$$J(\boldsymbol{\theta}) = \frac{\varepsilon^2}{2} = \frac{\left(\delta V + \boldsymbol{\theta}^{\mathrm{T}}\,\phi\right)^2}{2} \tag{8}$$

The gradient of this cost function in parameter space is:

$$\nabla_{\boldsymbol{\theta}} J = \varepsilon\,\nabla_{\boldsymbol{\theta}}\,\varepsilon = \varepsilon\,\phi \tag{9}$$

The minimizing trajectory in parameter space is then given by the opposite of the gradient multiplied by an *adaptive gain* matrix Γ:

$$\dot{\boldsymbol{\theta}} = -\Gamma\,\nabla_{\boldsymbol{\theta}} J = -\Gamma\,\varepsilon\,\phi \tag{10}$$

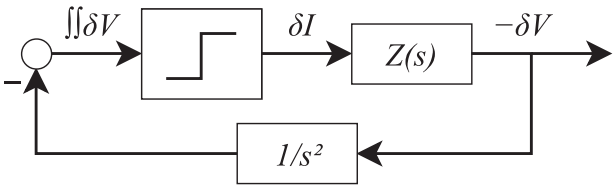

Fig. 5 − Relay feedback modified with double integrator in the loop.

Please cite this article as: Halvorsen IJ et al., Electrochemical low-frequency impedance spectroscopy algorithm for diagnostics of PEM fuel cell degradation, International Journal of Hydrogen Energy, https://doi.org/10.1016/j.ijhydene.2019.04.004

Γ is symmetric and positive definite, and we can choose it for simplicity to be diagonal:

$$\Gamma = \begin{bmatrix} \gamma_R & 0 \\ 0 & \gamma_V \end{bmatrix} \tag{11}$$

Inserting the definition of Γ into vector equation (10), the following two equations result:

$$\dot{R}_{LF} = -\gamma_R \overbrace{(\delta V + R_{LF}\,\delta I + V_{bias})}^{\varepsilon}\,\delta I \tag{12}$$

$$\dot{V}_{bias} = -\gamma_V\,(\delta V + R_{LF}\,\delta I + V_{bias}) \tag{13}$$

These two equations can be calculated online to track the parameters. Tuning γ_R and γ_V is a separate control engineering task: they can be chosen from a wide range, with larger values improving convergence but reducing stability.

The gradient algorithm can be easily implemented as a block diagram as depicted in Fig. 6, requiring nothing more than sums, multiplications, and memory storage of the two integrator states.

The bias estimate will be subtracted from the measured δV before this is fed back to the relay, so the tuning parameters must be adjusted with some care to avoid inducing instabilities. Supplying a reasonable estimate for the LFR as an initial value will give a faster start-up.

Estimation of LFR

The purpose of this gradient algorithm developed in section Compensation of voltage bias was to estimate the voltage bias and use it online to ensure a symmetric relay limit cycle; however, this method also outputs a direct online estimate of the LFR.

Due to the continuous cycling, there will be some noise in this online LFR estimate. To obtain a reliable estimate complete with standard deviation, it is advisable to apply the least-squares method on a number of full relay cycles once the limit cycle has been reached; this calculation can be performed offline after the test has been completed.

The LFR frequency, f_{LFR}, has been identified by Rezaei Niya et al. [15] as a relevant measurement to diagnose GDL flooding: in such a condition, f_{LFR} would be significantly lower than expected. This frequency can be readily calculated by measuring the duration of an appropriate number of relay cycles once the limit cycle has been reached, and taking the average and standard deviation of their inverse.

The fuel cell impedance profile, including the LFR, depends strongly on operating conditions. To provide comparable results, relay feedback must be carried out at the same conditions of current, temperature, humidity, excess ratio etc. While methods to compensate for the effect of different operating conditions on the LFR may be developed, they are beyond the scope of this article.

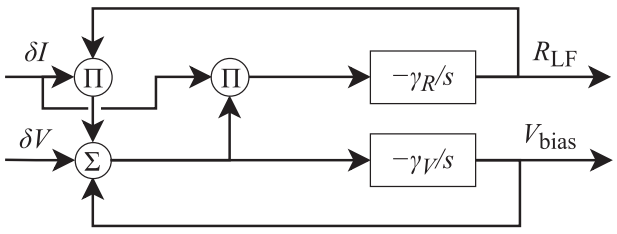

Fig. 6 – Implementation of the gradient algorithm for parameter estimation.

Results and discussion

A simulation model is implemented in Simulink™ according to the model shown in Fig. 7, and the calculations are performed in Matlab™. The impedance model of the fuel cell is implemented from the fitted electrical equivalent model in Fig. 1 with the parameters shown in Table 1.

The Nyquist diagram for the impedance model of a single cell is shown in Fig. 8; as this is drawn, as customary, with a reversed imaginary axis, a point below the real axis actually represents a positive phase. The plot starts at steady-state (marked with ◦) around 6.8 mΩ, bends downwards (i.e. towards positive phase), hits the real axis again at the point of interest, which is the low frequency intercept at 8.3 mΩ (marked with green ∗). The curve is completed up to infinite frequency at the high frequency intercept (marked with magenta ∗). The excitation experiments are around the low frequency intercept at 2.2 rad/s = 0.35 Hz. The identified point from the simulation (red ⋄) fits quite well to the real value; note that this resistance estimate is calculated by a least-square fit on the reasonably steady oscillating periods in the last half of the experiment. This will be typically an off-line procedure that may be applied if the data are logged and stored, e.g with 10 ms sample time. For a real-time implementation, the bias and resistance estimator offer an alternative recursive algorithm that is easy to implemented and does not require access to logged data.

In Fig. 9 the Bode diagram for $Z(s)/s^2$ is shown. The phase has the same shape as for $Z(s)$, but is shifted down by -180°. The gain margin (G_m) is 55.3 dB = 582 at the critical frequency ω_{180}. The Bode diagram has exactly the same phase behaviour around -180° as in the Nyquist diagram around zero in Fig. 8. The gain (logarithmic dB units) and phase is plotted as a function of angular frequency (logarithmic). The gain margin represents the ultimate gain for $Z(s)/s^2$, so from this the low frequency resistance can alternatively be calculated as $R_{LF} = \omega_{180}^2/G_m = 2.2^2/582 = 8.3\,m\Omega$. An interesting property around the zero phase frequency of $Z(s)$ (the -180° of $Z(s)/s^2$) is that the phase has close to linear relation with the logarithmic angular frequency. This may be exploited for final adjustments of the estimated properties of the low frequency intercept if the resulting phase during an experiment is found to be close to, but not exactly zero.

Fig. 10 shows the result of a 60 s simulation. In the bottom plot, the modelled voltage (equation (7)) from the bias estimator (red) fits the measured voltage (blue) quite well after the convergence of the estimated resistance during the first few cycles.

The resulting estimates for the resistance R_{LF} and voltage bias V_{bias} are shown in Fig. 11. The estimator of Fig. 6 is implemented in Simulink and connected to the relay excitation feedback loop as illustrated in Fig. 7. Observe the small variation due to the noise and the cycling. For a more precise

Please cite this article as: Halvorsen IJ et al., Electrochemical low-frequency impedance spectroscopy algorithm for diagnostics of PEM fuel cell degradation, International Journal of Hydrogen Energy, https://doi.org/10.1016/j.ijhydene.2019.04.004

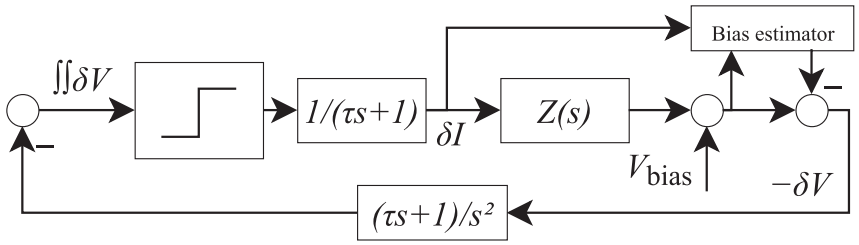

Fig. 7 – The full model as implemented in Simulink. The $(\tau s + 1)$ elements represent actuator dynamics and their compensation (section Actuator dynamics), whereas the *Bias estimator* block is the subdiagram of Fig. 6.

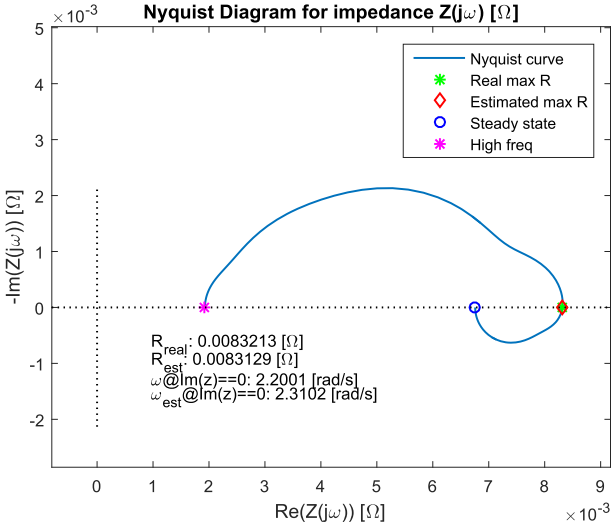

Fig. 8 – Nyquist diagram for the impedance model of the fuel cell.

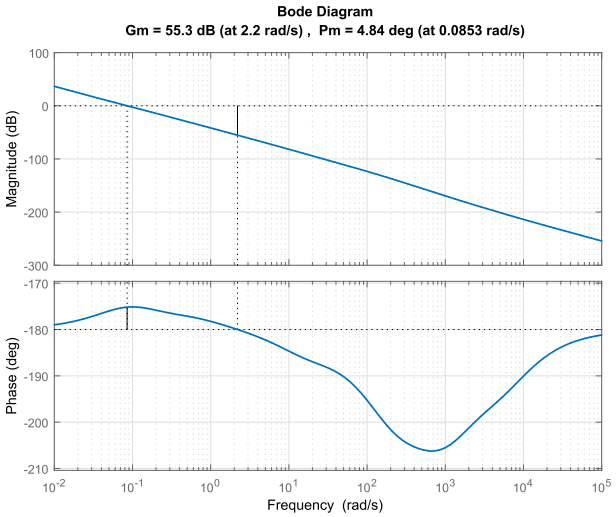

Fig. 9 – Bode diagram with gain and phase margins for $\mathbf{Z(s)/s^2}$.

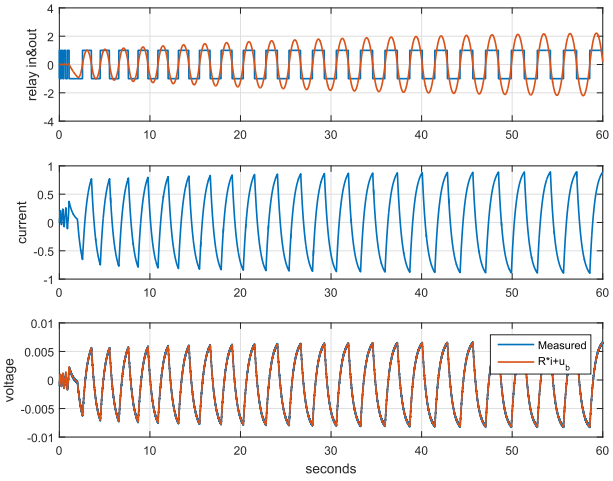

Fig. 10 – Top: relay input ($\times$ 1000) (red) and output (blue square wave). Middle: current. Bottom: measured and estimated voltage (almost overlaid). (For interpretation of the references to color in this figure legend, the reader is referred to the Web version of this article.)

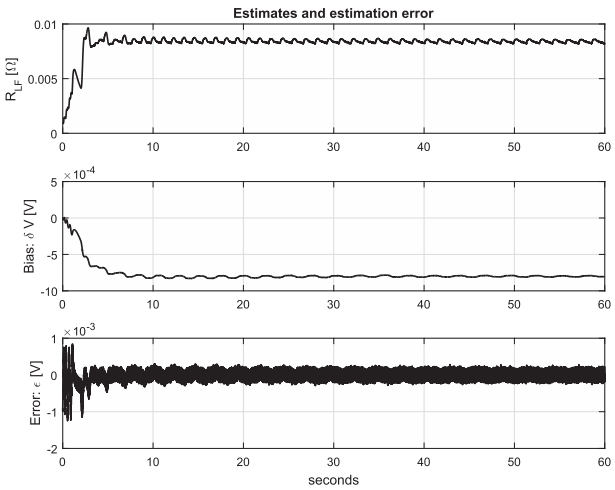

Fig. 11 – Online estimates for resistance (top), voltage bias (middle), and estimation error (bottom) which is the difference between estimated cell voltage and measured voltage.

estimate, the offline least-squares solution may be used, or simply a low-pass filter may be applied to the last, reasonably steady part of the LFR estimator signal. The estimation error ε being close to white noise plus the cyclic excitation indicates reasonable convergence of the estimates. The estimated LFR cycles between 8.2 mΩ to 8.6 mΩ, which is close to the known value of 8.3 mΩ.

Please cite this article as: Halvorsen IJ et al., Electrochemical low-frequency impedance spectroscopy algorithm for diagnostics of PEM fuel cell degradation, International Journal of Hydrogen Energy, https://doi.org/10.1016/j.ijhydene.2019.04.004

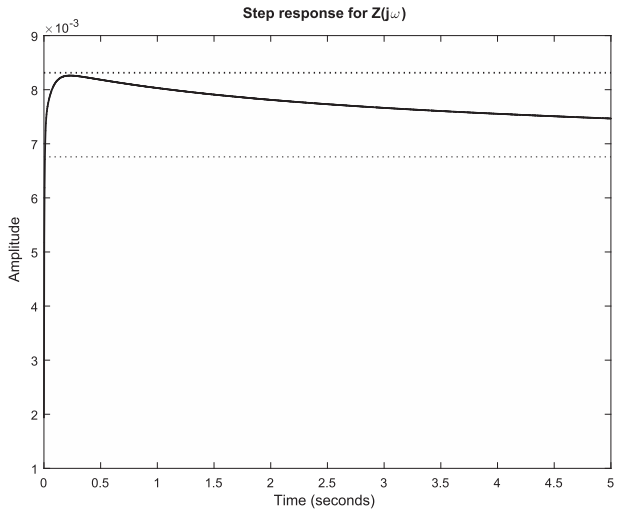

Fig. 12 – Open-loop voltage response for one A step in current through $Z(s)$.

Fig. 12 shows the voltage response for a (negative) unit step in current. A very interesting observation is that the overshoot peak is almost exactly equal to $R_{LF}\,\delta I$ (the higher dotted line): this may actually be used directly as an estimator of the LFR, assuming a sufficiently fast and noise-free sampling of voltage is available (at least 10 Hz in this example). Note also the rather slow decay towards steady state (the lower dotted line): the settling time is in fact longer than 5 min, which implies that during the relay feedback, with oscillations with periods of around 3 s, steady state is far from being reached. It will not be so easy to determine the peak accurately on a realistically noisy voltage measurement, so using a single step and measure the peak is not directly applicable in practice.

Practical implications

In practice, the relay feedback algorithm will start by itself when the loop is closed, just triggered by noise. In the simulations, where an ideal relay is used, a short step in current in the beginning kicks the feedback loop into its cycling operation; the initial values of both integrators are set to zero. Presence of measurement noise may lead to some rapid high frequency zero crossings of the feedback signal and lead to corresponding fast relay switching, as visible at early times in Fig. 10. This can be avoided in practical operation by a simple hysteresis function, or limiting the shortest switching time in the relay logic.

Results show that the proposed method is fast, robust, precise and accurate. However, it is vital that the fuel cell control system has a sufficiently fast sampling rate, e.g. 10 ms–20 ms, and that the load can be controlled by the DC/DC promptly upon demand during the experiment. The schedule of such experiments during normal fuel cell operation must be assessed for each application type: e.g., in the GIANTLEAP project [32], the fuel cell system acts as a charger to an electrical bus battery, and it is easy to execute this kind of function anytime when the bus battery charge status is somewhere between 30% and 70%.

Ideally, the algorithm should be run at the same set of fuel cell operating conditions every time, but this is probably not achievable in practical operation. This calls for correlations of the fuel cell impedance model and operating conditions like current, temperature, pressure and other relevant parameters. When the estimated data is meant to be used for prognostics and health monitoring, it is important that the fuel cell system operating state is stored along with the estimator results, such that a suitable normalization can be applied.

The necessary perturbations are rather small, so that such experiments should not lead to any additional degradation of the fuel cells.

The estimation algorithm may be tweaked by adjusting its parametersΓ. It is further recommended to filter both the current and voltage measurements with identical low-pass filters for removal of noise and high-frequency components of the signals fed to the estimator.

Alternative approaches

The proposed relay-feedback method is fast and robust, but there are other possible identification approaches.

An approach not requiring online feedback is to apply perturbations at a set of frequencies around the expected one; for each frequency, phase and magnitude can be calculated by means of Fourier analysis of the time series. It is then possible to estimate f_u by interpolation; μ_u can either be found by another interpolation on the available data, or by an additional experiment at the now known f_u.

A method that is related to the relay feedback is the phase-locked loop (PLL) [33], which may overcome issues with time lags. The PLL consists of algorithms for a phase detector, a frequency-controlled oscillator and a control function for adjusting the frequency to obtain the desired phase. The bias compensation can be applied for this methods as well.

Experiments should be as short as possible to reduce the impact of slow parameter drift (temperature, humidity, etc.) and to minimise the disruption to system operation. The relay excitation method, by virtue of its simplicity, is faster than separate frequency interpolation and PLL.

Conclusion

A simple algorithm based on relay feedback has been proposed to measure the low-frequency intercept of the EIS spectrum of fuel cells; the proposed method has been tested in simulations, indicating the ability to converge to a solution within 10 s and in spite of both bias and random noise in the voltage measurement. The parameters estimated by the method, i.e. the LFR and its associated frequency, are only observable in dynamic or transient operation, and it is necessary to induce sufficient perturbations to identify these parameters; this kind of characterization is normally performed in laboratories, e.g. with a full EIS.

However, when the fuel cell is a part of a deployed power production system, the use of laboratory methods like EIS is normally not available: the contribution from this paper is a method for dynamic parameter characterization that can be included in real-world fuel cell applications to improve the

Please cite this article as: Halvorsen IJ et al., Electrochemical low-frequency impedance spectroscopy algorithm for diagnostics of PEM fuel cell degradation, International Journal of Hydrogen Energy, https://doi.org/10.1016/j.ijhydene.2019.04.004

information about state of health and ageing of fuel cells. The algorithm requires only simple operations (comparison, sum, multiplication) and storage of just four floating-point numbers (two in the relay feedback's integrators, and two in the estimator subsystem): it is therefore appropriate for online implementation in a commercial system for continuous monitoring of the state of health of fuel cells.

The main uncertainty of this method is related to the actuating characteristics of the load current control, so it is expected that some adaptions may be required based on results from realistic experiments. Testing on single cells and stacks are in progress within the GIANTLEAP project, and the algorithm is planned to be included in the GIANTLEAP prototype.

Acknowledgements

This project has received funding from the Fuel Cells and Hydrogen 2 Joint Undertaking under grant agreement No. 700101. This Joint Undertaking receives support from the European Union's Horizon 2020 research and innovation programme and Hydrogen Europe and N.ERGHY. Ivan Pivac acknowledges the support from the Croatian Science Foundation (contract DOK-2014-06-4783).

Notation

a	Oscillation amplitude, [V]
C	Areal capacitance, $[F/cm^2]$
d	Relay amplitude, $[A/cm^2]$
f	Frequency, [Hz]
I	Current density, $[A/cm^2]$
j	Imaginary unit ($j = \sqrt{-1}$)
J	Cost function, $[V^2]$
L	Areal inductance, $[H\ cm^2]$
R	Areal resistance, $[\Omega\ cm^2]$
s	Laplace variable, [rad/s]
V	Voltage, [V]
Z	Areal impedance, $[\Omega\ cm^2]$
γ_R	LFR adaptive gain, $[A^{-2}]$
γ_V	Bias adaptive gain, [–]
μ	Process gain, [Ω]
τ	Time constant, [s]
ε	Model error, [V]
$\boldsymbol{\theta}$	Parameter vector
ϕ	Model structure vector
ω	Angular velocity ($\Omega = 2\pi f$), [rad/s]
$\dot{\circ}$	Time derivative, $[s^{-1}]$

REFERENCES

[1] Fuel cells and hydrogen Joint undertaking. Multi-annual work plan; 2014. URL, http://www.fch.europa.eu/sites/default/files/documents/FCH2%20JU%20-%20Multi%20Annual%20Work%20Plan%20-%20MAWP_en_0.pdf.
[2] Wu J, Yuan XZ, Martin JJ, Wang H, Zhang J, Shen J, Wu S, Merida W. A review of PEM fuel cell durability: degradation mechanisms and mitigation strategies. J Power Sources 2008;184:104–19.
[3] Buchi FN, Inaba M, Schmidt TJ. Polymer electrolyte fuel cell durability. Springer; 2009.
[4] Mench MM, Kumbur EC, Veziroglu TN. Polymer electrolyte fuel cell degradation. Elsevier; 2011.
[5] De Bruijn FA, Dam VAT, Janssen GJM. Review: durability and degradation issues of PEM fuel cell components. Fuel Cells 2008;8(1):3–22.
[6] Nara H, Tominaka S, Momma T, Osaka T. Impedance analysis counting reaction distribution on degradation of cathode catalyst layer in PEFCs. J Electrochem Soc 2011;158(9):B1184–91.
[7] Saleh FS, Easton EB. Diagnosing degradation within PEM fuel cell catalyst layers using electrochemical impedance spectroscopy. J Electrochem Soc 2012;159(5):B546–53.
[8] Saleh FS, Easton EB. Assessment of the ethanol oxidation activity and durability of Pt catalysts with or without a carbon support using electrochemical impedance spectroscopy. J Power Sources 2014;246:392–401.
[9] Reid O, Saleh FS, Easton EB. Determining electrochemically active surface area in PEM fuel cell electrodes with electrochemical impedance spectroscopy and its application to catalyst durability. Electrochim Acta 2013;114:278–84.
[10] Zhang W, Maruta T, Shironita S, Umeda M. Anode and cathode degradation in a PEFC single cell investigated by electrochemical impedance spectroscopy. Electrochim Acta 2014;131:245–9.
[11] Pivac Ivan, Bezmalinović Dario, Barbir Frano. Catalyst degradation diagnostics of proton exchange membrane fuel cells using electrochemical impedance spectroscopy. Int J Hydrogen Energy 2018;43(29):13512–20.
[12] Nonobe Y. Development of the fuel cell vehicle mirai. IEEJ Trans Electr Electron Eng 2017;12:5–9.
[13] Engebretsen E, Robinson JB, Obeisun O, Mason T, Finegan D, Hinds G, Shearing PR, Brett DJ. Electro-thermal impedance spectroscopy applied to an open-cathode polymer electrolyte fuel cell. J Power Sources 2016;302:210–4.
[14] Engebretsen E, Mason TJ, Shearing PR, Hinds G, Brett DJ. Electrochemical pressure impedance spectroscopy applied to the study of polymer electrolyte fuel cells. Electrochem Commun 2017;75:60–3.
[15] Niya Seyed Mohammad Rezaei, Phillips Ryan K, Hoorfar Mina. Process modeling of the impedance characteristics of proton exchange membrane fuel cells. Electrochim Acta 2016;191:594–605.
[16] Pivac Ivan, Šimić Boris, Barbir Frano. Experimental diagnostics and modeling of inductive phenomena at low frequencies in impedance spectra of proton exchange membrane fuel cells. J Power Sources 2017;365:240–8.
[17] Pivac Ivan, Barbir Frano. Inductive phenomena at low frequencies in impedance spectra of proton exchange membrane fuel cells–a review. J Power Sources 2016;326:112–9.
[18] Dhirde AM, Dale NV, Salehfar H, Mann MD, Han T-H. Equivalent electric circuit modeling and performance analysis of a pem fuel cell stack using impedance spectroscopy. IEEE Trans Energy Convers 2010;25:778–86.
[19] O'hayre R, Cha S, Colella W, Prinz FB. Fuel cell fundamentals. 2nd ed. NJ: John Wiley and Sons; 2009.
[20] Ren P, Pei P, Li Y, Wu Z, Chen D, Huang S, Jia X. Diagnosis of water failures in proton exchange membrane fuel cell with zero-phase ohmic resistance and fixed-low-frequency impedance. Appl Energy 2019;239:785–92.
[21] Jeppesen Christian, Simon Araya Samuel, Lennart Sahlin Simon, Juhl Andreasen Søren, Knudsen Kær Søren. An EIS alternative for impedance measurement of a high

Please cite this article as: Halvorsen IJ et al., Electrochemical low-frequency impedance spectroscopy algorithm for diagnostics of PEM fuel cell degradation, International Journal of Hydrogen Energy, https://doi.org/10.1016/j.ijhydene.2019.04.004

temperature PEM fuel cell stack based on current pulse injection. Int J Hydrogen Energy 2017;42(24):15851–60.
[22] Brunetto C, Moschetto A, Tina G. Pem fuel cell testing by electrochemical impedance spectroscopy. Electr Power Syst Res 2009;79:17–26.
[23] Manganiello P, Petrone G, Giannattasio M, Monmasson E, Spagnuolo G. Fpga implementation of the eis technique for the on-line diagnosis of fuel-cell systems. 2017 IEEE 26th International Symposium on Industrial Electronics; 2017. p. 981–6.
[24] Debenjak A, Boškoski P, Musizza B, Petrovčič J, Juričič Đ. Fast measurement of proton exchange membrane fuel cell impedance based on pseudo-random binary sequence perturbation signals and continuous wavelet transform. J Power Sources 2014;254:112–8.
[25] Aroge FA, Barendse PS. Time-frequency analysis of the chirp response for rapid electrochemical impedance estimation. 2018 IEEE Energy Conversion Congress and Exposition; 2018a. p. 2047–52.
[26] Debenjak A, Jovan V, Petrovčič J, Gašperin M, Pregelj B. An assessment of water conditions in a pem fuel cell stack using electrochemical impedance spectroscopy. Proceedings of the IEEE 2012 Prognostics and System Health Management Conference; 2012. p. 1–6.
[27] Aroge FA, Barendse PS. Signal injection by active load modulation for pem fuel cell diagnostics. 2018 IEEE PES/IAS PowerAfrica; 2018b. p. 7–12.
[28] Petrone Raffaele. Electrochemical impedance spectroscopy for the on-board diagnosis of PEMFC via on-line identification of equivalent circuit model parameters. PhD thesis. Università di Salerno & Université de Franche-Comté, Salerno & Belfort; 2014.
[29] Russo Luigi, Sorrentino Marco, Polverino Pierpaolo, Pianese Cesare. Application of Buckingham π theorem for scaling-up oriented fast modelling of proton exchange membrane fuel cell impedance. J Power Sources 2017;353:277–86.
[30] Åström Karl Johan, Hägglund Tore. PID controllers: theory, design, and tuningvol. 2. , NC: Instrument society of America Research Triangle Park; 1995.
[31] Ioannou Petros A, Sun Jing. Robust adaptive controlvol. 1. Upper Saddle River, NJ: PTR Prentice-Hall; 1996.
[32] EU project ID 700101. Website of the Giantleap project. 2018. http://giantleap.eu.
[33] Abramovitch D. Phase-locked loops: a control centric tutorial. In: Proceedings of the 2002 American control conference (IEEE cat. No.CH37301). vol. 1; May 2002. p. 1–15. https://doi.org/10.1109/ACC.2002.1024769. vol.1.

Please cite this article as: Halvorsen IJ et al., Electrochemical low-frequency impedance spectroscopy algorithm for diagnostics of PEM fuel cell degradation, International Journal of Hydrogen Energy, https://doi.org/10.1016/j.ijhydene.2019.04.004